THE JOURNAL OF BIOLOGICAL CHEMISTRY VOL. 283, NO. 11, pp. 7271–7279, March 14, 2008

Homophilic Interactions of the Amyloid Precursor Protein (APP) Ectodomain Are Regulated by the Loop Region and Affect β-Secretase Cleavage of APP*[S]

Received for publication, September 26, 2007, and in revised form, December 13, 2007 Published, JBC Papers in Press, January 8, 2008, DOI 10.1074/jbc.M708046200

Daniela Kaden[‡1], Lisa-Marie Munter[‡1], Mangesh Joshi[§], Carina Treiber[‡], Christoph Weise[‡], Tobias Bethge[‡], Philipp Voigt[¶], Michael Schaefer[¶], Michael Beyermann[§], Bernd Reif[§], and Gerd Multhaup[‡2]

From the [‡]Institut für Chemie und Biochemie, Freie Universität Berlin, 14195 Berlin, Germany, the [§]Leibniz-Institut für Molekulare Pharmakologie, 13125 Berlin, Germany, and the [¶]Molekulare Pharmakologie und Zellbiologie, Neurowissenschaftliches Forschungszentrum, Charité Universitätsmedizin Berlin, 14195 Berlin, Germany

We found previously by fluorescence resonance energy transfer experiments that amyloid precursor protein (APP) homodimerizes in living cells. APP homodimerization is likely to be mediated by two sites of the ectodomain and a third site within the transmembrane sequence of APP. We have now investigated the role of the N-terminal growth factor-like domain in APP dimerization by NMR, biochemical, and cell biological approaches. Under nonreducing conditions, the N-terminal domain of APP formed SDS-labile and SDS-stable complexes. The presence of SDS was sufficient to convert native APP dimers entirely into monomers. Addition of an excess of a synthetic peptide (APP residues 91–116) containing the disulfide bridge-stabilized loop inhibited cross-linking of pre-existing SDS-labile APP ectodomain dimers. Surface plasmon resonance analysis revealed that this peptide specifically bound to the N-terminal domain of APP and that binding was entirely dependent on the oxidation of the thiol groups. By solution-state NMR we detected small chemical shift changes indicating that the loop peptide interacted with a large protein surface rather than binding to a defined pocket. Finally, we studied the effect of the loop peptide added to the medium of living cells. Whereas the levels of α-secretory APP increased, soluble β-cleaved APP levels decreased. Because Aβ40 and Aβ42 decreased to similar levels as soluble β-cleaved APP, we conclude either that β-secretase binding to APP was impaired or that the peptide allosterically affected APP processing. We suggest that APP acquires a loop-mediated homodimeric state that is further stabilized by interactions of hydrophobic residues of neighboring domains.

The amyloid precursor protein (APP)[3] of Alzheimer disease is one of the best studied type I cell surface glycoproteins with a proposed regulatory role in cell adhesion in the peripheral and central nervous system (1). APP is physiologically processed by either α- or β-secretases, which release the soluble ectodomain (sAPPα or sAPPβ) from the cell surface (2–5). Alternatively, the membrane-bound fragment APP-C-terminal fragment, which is derived from β-secretase cleavage, is further processed by the γ-secretase into the cytoplasmic domain of APP and amyloid β-peptides (Aβ) of varying lengths (6–9). Recently, elucidation of the γ-secretase cleavage mechanism has revealed that a conserved *GXXXG* motif in the transmembrane sequence of APP mediates homophilic helix-helix interactions and has an important role in the processing of Aβ40/42 into shorter Aβ species, *i.e.* Aβ38, Aβ37, Aβ35, and Aβ34 (7).

Unraveling structural features of APP by NMR spectroscopy and x-ray crystallography has led to the identification of specific regions that function as subdomains (see Fig. 1*A*). The extracellular N-terminal domain of APP has been dissected into the E1 region consisting of the N-terminal growth factor-like domain (GFLD) followed by the copper-binding domain (CuBD) (10). An acidic region (residues 190–264) precedes the carbohydrate domain, which contains the *N*-glycosylation site of the ectodomain (11). The carbohydrate domain together with the juxtamembrane region (residues 507–589) is called E2 or the central APP domain (12).

The homophilic binding between extracellular and transmembrane domains of APP is of considerable interest because of possible implications in its functional role and regulatory aspects for APP processing into Aβ peptides. We and others have shown previously that APP and other substrates of the γ-secretase (*e.g.* ErbB-4 and E-cadherin) can form homodimers (13–19). A rough quantification of APP homodimerization in living higher eukaryotic cells by fluorescence resonance energy transfer analysis yielded about 30% APP homodimers of total membrane-bound APP (7). APP homodimerization is likely to be mediated by three different sites (7). Two sites located within the ectodomain of APP are believed to be of critical importance

* This work was supported by the Deutsche Forschungsgemeinschaft (DFG) and the Breuer Stiftung. The costs of publication of this article were defrayed in part by the payment of page charges. This article must therefore be hereby marked "*advertisement*" in accordance with 18 U.S.C. Section 1734 solely to indicate this fact.

[S] The on-line version of this article (available at http://www.jbc.org) contains supplemental "Materials and Methods," Figs. 1–3, and references.

[1] Both authors contributed equally to this work.

[2] To whom correspondence should be addressed: Institut für Chemie und Biochemie, Freie Universität Berlin, Thielallee 63, 14195 Berlin, Germany. Tel.: 49-30-838-55533; Fax: 49-30-838-56509; E-mail: multhaup@chemie.fu-berlin.de.

[3] The abbreviations used are: APP, amyloid precursor protein; Aβ, amyloid β-peptide; sAPPα/β, secreted or soluble APP ectodomain, α- or β-cleaved; GFLD, growth factor-like domain; CuBD, copper-binding domain; KPI, Kunitz-type protease inhibitor; AOX, alcohol oxidase; ELISA, enzyme-linked immunosorbent assay; DTSSP, dithiobis(sulfosuccinimidyl) propionate; Fmoc, *N*-(9-fluorenyl)methoxycarbonyl; GPC, gel permeation chromatography; MALDI, matrix-assisted laser desorption ionization; HPLC, high pressure liquid chromatography; PBS, phosphate-buffered saline; BACE, β-site APP cleaving enzyme; MAPK, mitogen-activated protein kinase; WT, wild type; mut, mutant.

for homodimerization of full-length APP (7, 12, 17, 18), *i.e.* the loop region encompassing residues 91–111 and a second site overlapping with the collagen binding site spanning residues 448–465 (13, 16, 17, 19). The third site is localized within the transmembrane sequence of APP and determines on γ-secretase cleavages but leaves dimerization of full-length and secreted APP unaffected (7).

The homophilic binding mechanism of APP is still a subject of debate. In this study, we explored the proposed N-terminal site of APP dimerization and its impact on APP processing. NMR, biochemical, and cell biological approaches were applied to elucidate the involvement of the disulfide bridge-stabilized (between Cys-98 and Cys-105) loop and its basic residues in the dynamics of the conformation and APP cleavage by secretases.

MATERIALS AND METHODS

Plasmids and Transfections—For stable expression of APP, the plasmid pCEP4 (Invitrogen) containing the cDNA of APP695 was used as described previously (7) and transfected into SH-SY5Y cells (ATCC CRL-2266, Manassas, VA) using Transfectin (Bio-Rad) following the manufacturer's instructions. Cloning, expression, and enrichment of the β-site APP cleaving enzyme (BACE) ectodomain were performed as described previously (20).

Loop Peptide Synthesis—The wild type (WT) loop peptide (NWCKRGRKQCKTHPHFVIPYR) or peptide (PVTIQNWCKRGRKQCKTHPHFVIPYR) for NMR experiments containing intramolecular disulfide bridges formed by the indicated cysteine residues and a loop mutant (mut) control peptide containing Ser residues instead of Cys residues to inhibit the disulfide bond arrangement (NWSKRGRKQSKTHPHFVIPYR) were synthesized with the automated system ABI 433a (Applied Biosystems, Foster City, CA) on Trt-Tentagel resin (0.25 mmol/g, 0.5 g; Rapp-Polymere, Tübingen, Germany) using the Fmoc strategy (double couplings with 9 eq of Fmoc amino acids/(2-(1H-Benzotriazole-1-yl)-1,1,3,3-tetramethyluronium hexafluorophosphate/6 eq of *N*,*N*-diisopropylethylamine). After final cleavage/deprotection using trifluoroacetic acid/H_2O (9:1), crude peptides were purified by preparative reverse-phase HPLC to yield final products of 95% purity according to HPLC analysis (detector, 220 nm). For cyclization (disulfide formation), peptides (1 mg/ml) were dissolved in sodium bicarbonate buffer at pH 8.5, and the mixture was stirred while exposed to air for 3 days. After lyophilization, the crude product was purified by preparative HPLC and characterized by MALDI mass spectrometry, which gave the expected masses for the linear and cyclic peptides (see supplemental Fig. 1). For the experiments, loop-WT and loop-mut were dissolved in phosphate-buffered saline (PBS), 137 mM NaCl, 2.7 mM KCl, 10 mM Na_2HPO_4, 2 mM KH_2PO_4 at concentrations of 5 mg/ml, which equals concentrations of 2.06 mM loop-WT and 2.03 mM loop-mut, and further diluted as indicated in the individual experiment descriptions.

Sandwich Enzyme-linked Immunosorbent Assay (ELISA) and Western Blots—Stably transfected cells were plated at a density of 2.8×10^5 cells/12-well dish. The day after splitting, 200 μl of fresh medium (Opti-MEM, Invitrogen) supplemented with either vehicle control (PBS) or loop-WT or loop-mut peptides were added and incubated for 6 h. Aliquots of the conditioned medium were directly analyzed for secreted APP. Samples were separated by SDS-PAGE, transferred to nitrocellulose, and immunolabeled either with antibody W0-2 (21) to detect sAPPα or with antibody 879 (provided by P. Paganetti, Novartis) to detect sAPPβ. sAPPβ signals were densitometrically quantified using the Alpha Imager and suitable AlphaEase software (Alpha Innotech). For Aβ40- and Aβ42-specific ELISAs, 50 μl of medium were analyzed according to the manufacturer's instructions (The Genetics Company, Zurich). The same protocol was applied to determine sAPPα levels except that the anti-Myc antibody (Cell Signaling Technology) was used as the capture antibody.

BACE Activity Assay—The BACE ectodomain enriched by Q-Sepharose (GE Healthcare) ion exchange chromatography from supernatants of stably transfected HEK293 cells was concentrated with 30-kDa cut-off Amicon spin columns (Millipore). For the enzymatic reaction, 20 μl of soluble BACE (PBS or Dulbecco's modified Eagle's medium as control) were incubated in 100 μl of reaction buffer (100 mM NaAc, pH 5, 100 μM substrate) at room temperature with or without 25, 50, and 100 μM loop peptides. BACE activity was measured by quantifying cleavage of the fluorescent substrate Cy3-SEVNLDAEFK-(Cy5Q)-NH_2 (22).

Biacore Analysis—Surface plasmon resonance analysis (Biacore 3000, GE Healthcare) of peptide binding to APP18–350 was done at 25 °C in 1× PBS buffer without detergent at flow rates of 30 μl/min according to standard protocols provided by the manufacturer. Recombinant APP was coupled to a CM5 sensor chip via standard NHS/EDC activation chemistry (Biacore amine coupling kit) in amounts that yielded 1,600 response units. Peptides were dissolved (10 mg/ml in water), diluted to a working solution of 1 μg/μl, and injected at concentrations of 6–18 μg/ml for 1 min followed by a 10-min elution with the PBS buffer. The sensor chip was cleaned of immunocomplexes by the injection of 10 μl of regeneration solution (50 mM NaOH). The base lines for the curves shown in Fig. 4 were adjusted to zero for a better comparison of the results. Kinetic constants were obtained by fitting curves to a single-site binding model ($A + B = AB$) with mass transfer using the BIAevaluation 4.1 program (Biacore). The time frame from 90 to 125 s was used to calculate the association rate constant. For the dissociation rate constant, a time frame from 150 to 700 s was chosen.

Purification of Recombinant APP—APP18–350 was produced in *Pichia pastoris* using the inducible promotor of the alcohol oxidase (AOX) and purified as described previously (16, 17) with the following modifications. Briefly, recombinant APP-containing supernatant of the growth culture medium was first purified by anion exchange chromatography (Q-Sepharose, GE Healthcare) and eluted in 50 mM Tris, pH 6.8, by a linear NaCl gradient up to 1 M NaCl. APP-containing fractions were concentrated to 20% of the initial volume with Amicon centrifugal tubes (30-kDa cut-off, Millipore). Subsequently, the APP-containing solution was loaded onto a gel permeation chromatography (GPC) column (Superdex 200, GE Healthcare) in buffer containing 50 mM NaH_2PO_4 and 100 mM NaCl at pH 6.9. The column was calibrated with standard pro-

tein markers (gel filtration LMW and HMW calibration kits, GE Healthcare). Fractions were analyzed by SDS-PAGE followed by silver staining of the gel or Western blot analysis using monoclonal antibody 22C11 (23).

Chemical Cross-linking—Aliquots of 25–50 μg of purified APP18–350 (0.5–1 μg/μl) were incubated with either vehicle (PBS) or 8- and 16-molar excesses of loop-WT or loop-mut peptides for 60 min. The chemical cross-linking reagent dithiobis(sulfosuccinimidyl) propionate (DTSSP; Pierce) was freshly dissolved (10 mM in water) and added to a final concentration of 1 mM. Cross-linking was allowed to proceed for 30 min. The reaction was terminated by the addition of Tris-HCl (100 mM, pH 7.5). All reactions were performed at 24 °C. For immunoblotting, 0.6 μg of treated and control samples were separated by SDS-PAGE and stained with monoclonal antibody 22C11.

NMR Measurements—Isotopically enriched APP18–350 was expressed in *P. pastoris*. Using a rich yeast/peptone/dextrose medium, we obtained ~98 mg/liter purified APP18–350. In contrast, use of a $^{2}H,^{15}N,^{13}C$ isotopically enriched yeast nitrogen base minimal medium (0.67% yeast nitrogen base, 0.5% $(^{15}NH_4)_2SO_4$, 2% [^{13}C]glucose) yielded only 7 mg/liter purified APP18–350. Growth of *P. pastoris* in minimal medium was accompanied by a drastic reduction of the pH value, which was readjusted by adding 100 mM phosphate buffer. Furthermore, expression of APP18–350 could only be achieved upon addition of 0.2 mg/liter $CuSO_4$ to the growth medium. The expression of protein was induced by addition of 2% methanol to the medium. To avoid the suppression of promotors of the alcohol oxidases AOX1 and AOX2, cells were incubated in a medium containing 0.1% glycerol prior to induction. Purification of recombinant APP18–350 was achieved by hydrophobic interaction chromatography (phenyl-Sepharose, GE Healthcare) followed by gel permeation chromatography on Superdex 200 using a buffer containing 50 mM NaH_2PO_4 and 100 mM NaCl, pH 6.9. Fractions were analyzed by SDS-PAGE. The identity and integrity of APP were verified by Western blot analysis with monoclonal antibody 22C11 (23). The purified protein was relatively unstable and showed degradation bands after 1 week (~20%) as judged by SDS-PAGE under NMR conditions (20 mM phosphate buffer, 50 mM NaCl, pH 7.0, at 30 °C). All described NMR experiments were therefore performed using fresh protein and were recorded within 7 days after protein expression to ensure that the employed protein was constitutively intact.

All NMR experiments were recorded on a Bruker 600-MHz Avance spectrometer equipped with a triple channel cryoprobe. The temperature was set to 30 °C in all experiments. $^{1}H,^{15}N$ correlation experiments were recorded using a standard heteronuclear single quantum correlation employing WATERGATE for solvent suppression. For titration experiments, the typical APP18–350 protein concentration was on the order of 0.1 mM. The acquisition time in the direct dimension was restricted to 50 ms. A total of 256 increments were recorded in the indirect dimension.

Assignment of the protein resonances was achieved by recording ^{15}N-^{1}H transverse relaxation-optimized spectroscopy HNCACB and HNCOCB experiments (24) using uniformly ^{2}H-, ^{15}N-, and ^{13}C-labeled APP18–350. Spectra were acquired using 96 × 88 × 2048 real data points employing 32 scans per increment. Acquisition times in F1(^{15}N), F2($^{13}C^{\alpha/\beta}$), and F3($^{1}H^{N}$) were 10.5, 2.6, and 68 ms, respectively. The carrier frequencies were set to 120.6, 42.7, and 4.7 ppm in the F1, F2, and F3 dimensions, respectively. Data were processed using the Bruker Topspin software and analyzed employing the program Sparky 3 (T. D. Goddard and D. G. Kneller, University of California, San Francisco).

RESULTS

The Loop-WT Peptide Impairs APP-APP Interaction—In earlier studies we showed that the N-terminal domain of recombinant APP (residues 18–350) containing a disulfide-bonded loop is sufficient to form dimers and higher oligomers (17). To investigate the possible role of the N-terminal loop in APP homointeraction, we expressed APP18–350 in *P. pastoris* and purified the protein as described previously (Fig. 1*B*) (16, 17). To differentiate between the effects of the disulfide bond itself and the basic residues flanked by the Cys residues in the primary sequence, we used a synthetic peptide that is referred to as the loop-WT peptide. As a control, we used a loop-mut peptide where Cys residues were replaced by Ser residues. The formation of the disulfide bridge in the loop-WT peptide was confirmed by MALDI mass spectrometric analysis (supplemental Fig. 1).

Fractions containing native APP18–350 dimers were obtained in a final purification step by GPC on a calibrated Superdex 200 fast protein liquid chromatography column (Fig. 1*B*). At high sensitivity settings, when the APP dimer containing the peak (fractions 19–23) and the salt peak (fraction 27 and higher) were off-scale, peaks containing higher oligomers became visible. Proteins eluted in fractions 16–18 correspond to tetramers, fractions 12–15 to octamers, and fractions 5–11 to higher oligomers (Fig. 1*B*). Additionally, the oligomeric states observed by GPC could be verified by blue native gel electrophoresis (see supplemental Fig. 2). The determination of the protein content of collected fractions revealed that by far the majority of APP18–350 eluted as homodimers and that monomers were absent under the conditions used. The protein was essentially purified to homogeneity as determined by SDS-PAGE and silver staining (Fig. 1, *B* and *C*). Fractions loaded onto the gel stained by silver were also analyzed by MALDI mass spectrometric analysis (data not shown). Only residual amounts of the yeast AOX could be detected and are visible as a faint band at 75 kDa (Fig. 1*C*). This was because of high levels of AOX expression after the induction of APP18–350 controlled by the AOX promotor. A closer inspection of results obtained by GPC and by SDS-PAGE indicates that under nonreducing conditions and in the presence of SDS, APP dimers are easily converted into monomers, tetramers into dimers, and higher oligomers mainly into tetramers (Fig. 1*B*). We found that SDS has a considerable influence on the monomer-dimer equilibrium of APP in the absence of reducing agents. Homomeric APP complexes could be separated by GPC into SDS-stable tetramers and dimers, whereas APP dimers obtained under native conditions were fully converted into monomers in the presence of SDS (Fig. 1*B*). Thus, APP dimers exist in SDS-labile and SDS-stable forms, the latter of which are derived exclusively from higher oligomers. The finding that under reducing

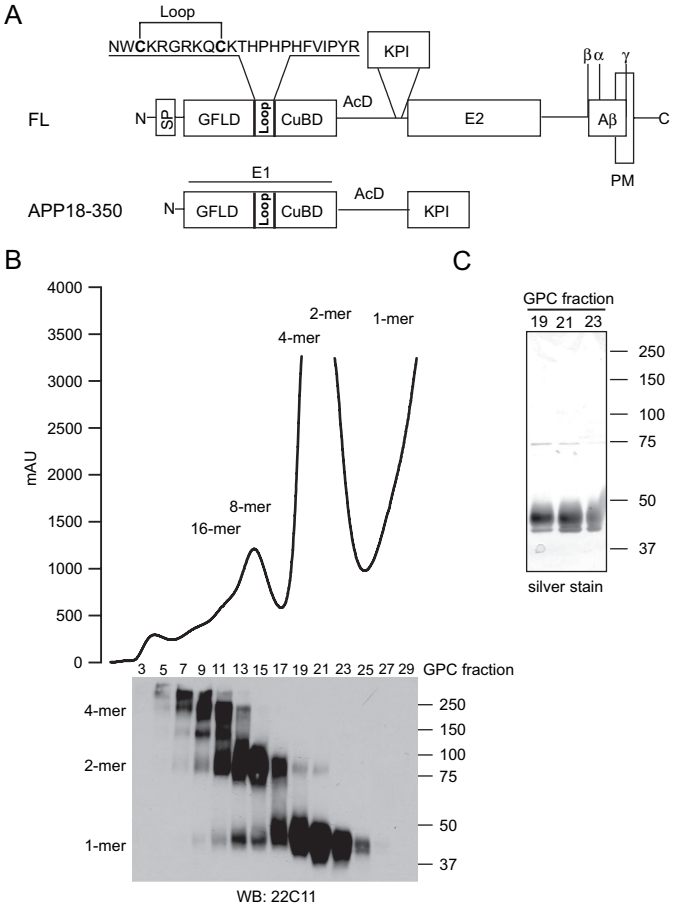

FIGURE 1. **APP18–350 homodimer is decreased upon addition of a molar excess of the loop-WT peptide.** *A*, schematic representations of full-length APP (*FL*) alternatively with (APP770) and without (APP695) the KPI domain and of recombinant APP18–350 as expressed in *P. pastoris* are shown. The loop sequence is *highlighted*. α, β, and γ indicate the cleavage sites of the respective secretases. *SP*, signal peptide; *AcD*, acidic domain; *PM*, plasma membrane. *B*, oligomers of recombinant APP18–350 were purified on a Q-Sepharose column and separated for the size with a Superdex 200 column. Fractions were analyzed for APP content by SDS-PAGE under nonreducing conditions and Western blot (*WB*) analysis with monoclonal antibody 22C11. The oligomerization state of APP18–350 as indicated in the chromatogram (*x*-mer) was calculated from the elution volume of the GPC and runs with seven different molecular mass standard proteins from 13.7 kDa (ribonuclease A) to 440 kDa (ferritin) (not shown). APP18–350 eluted exclusively as dimers and higher oligomers under native conditions. Note that no APP18–350 could be detected in the Western blot (*bottom panel*) in fractions where monomers are expected to elute according to the standards (*i.e.* fractions 27 and 29). Aliquots of GPC fractions (*numbers* as indicated on *top* of the *blot*) subjected to SDS-PAGE and Western blotting showed SDS-stable dimers, tetramers, and few higher oligomers derived from GPC fractions containing the next higher molecular mass forms. Native APP eluting at the position of the dimer was mainly converted into monomers under nonreducing conditions. *mAU*, milli absorption unit. *C*, proteins contained in fractions 19, 21, and 23 were separated by nonreducing SDS-PAGE and silver-stained. The recombinant APP could be purified essentially to homogeneity. *D*, dimer-containing fractions (fractions 19–23) were treated with (+) or without (−) 1 mM DTSSP. DTSSP yielded ~20% dimers (90 kDa) and small amounts of tetramers (*lanes DTSSP* and *Loop-WT*) in nonreducing SDS-PAGE; the majority was converted into monomers by SDS (45 kDa). Covalent cross-linking of APP18–350 could be inhibited in a concentration-dependent manner by the loop-WT peptide (*lanes DTSSP* and *Loop-WT* in 8- or 16-fold molar excess, denoted as *8* or *16*, respectively) but not by the loop-mut peptide (*lanes DTSSP* and *Loop-mut* in 8- or 16-fold molar excess). APP18–350 was immunodetected using monoclonal antibody 22C11. The oligomerization state of APP is indicated on the *left side* of the blots, and molecular mass markers are on the *right side* of the blots.

conditions all forms of APP were entirely converted into monomers (data not shown) indicates that covalent intramolecular linkages as provided by Cys-98 and Cys-105 forming the disulfide bridge are required to stabilize a dimerization-prone conformation of APP. Although we cannot exclude that other disulfide bridges occurring in APP (residues 18–350) may contribute to oligomerization, we rather assume that hydrophobic interactions are involved. This view is also supported by the NMR data described below.

To study specific effects of the loop peptide on dimerization of APP, fractions containing SDS-labile dimers (fractions 19–23) (Fig. 1*B*) were treated in the presence and absence of the loop peptide with DTSSP. DTSSP is a homobifunctional reagent that cross-links primary amines. After cross-linking, mainly dimers and low amounts of tetramers of APP became visible after SDS-PAGE and Western blotting but were not observed without the cross-linker (Fig. 1*D*). When reactions were performed with an 8- or 16-fold molar excess of the loop-WT peptide, the intensities of the dimer band (90 kDa) and the band representing tetramers (180 kDa) were weakened (Fig. 1*D*). Addition of the loop-WT peptide, but not the loop-mut peptide (Fig. 1*D*), inhibited the formation of covalently linked dimers and oligomers by affecting the monomer-dimer equilibrium of APP18–350. Thus, given that the dimers are not the result of intermolecular disulfide bridges, we conclude that the disulfide-bonded loop plays a crucial role in the noncovalent dimerization of APP.

The Loop-WT Peptide Drastically Reduces Aβ Secretion—To investigate the possibility that the loop-WT peptide, which has been shown to modulate the conformation of recombinant APP (Fig. 1 and see Fig. 5), can have an influence on cellular APP, we incubated living cells with the synthetic peptide. We examined whether the loop-WT and loop-mut peptides could alter APP processing and generation of Aβ. SH-SY5Y cells stably expressing APP695WT were tested for α- or β-secretase activities (Fig. 2, *A–D*) by measuring soluble APP levels (sAPPα and sAPPβ) in the presence and absence of the loop-WT peptide. Western blot analysis with polyclonal antibody 879 for sAPPβ and the monoclonal W0-2 for sAPPα revealed that sAPPα levels remained unchanged whereas sAPPβ decreased. A closer inspection with a sandwich ELISA showed that sAPPα levels increased upon the addition of a micromolar concentration of the synthetic loop-WT peptide to the medium (Fig. 2*B*). Densitometric quantification of sAPPβ and quantification of sAPPα by ELISA analysis indicated that APP cleavage by BACE was concomitantly impaired, although the maximum increase of sAPPα by 115% was not significant. Increasing concentra-

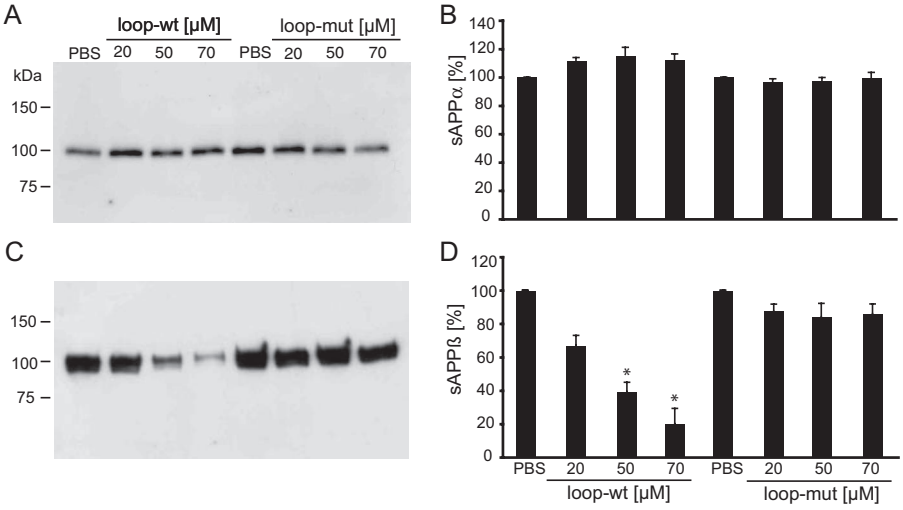

FIGURE 2. **Loop peptide selectively affects β-secretase cleavage.** APP-expressing SH-SY5Y cells were treated with vehicle (PBS) or increasing amounts of loop-WT or loop-mut peptide for 6 h, and conditioned media were analyzed. *A*, Western blot of sAPPα stained with monoclonal antibody W0-2. *B*, quantification of sAPPα by ELISA. The addition of the loop-WT peptide (concentrations as indicated) yielded an increase of sAPPα up to 115%. The vehicle control was set as 100% (means ± S.E., $n = 4$). *C*, Western blot of sAPPβ stained with polyclonal antibody 897. *D*, quantification of sAPPβ by densitometric analysis of Western blots from independent experiments (means ± S.E., $n = 3$). The addition of the loop-WT peptide showed a concentration-dependent reduction of sAPPβ. *Asterisks* indicate significant differences with the PBS buffer control ($p < 0.01$, Student's *t* test).

tions of the loop peptide added to the medium (20, 50, and 70 μM) reduced sAPPβ levels by 33, 61, and 80%, respectively (Fig. 2, *C* and *D*). Based on the fact that the α-secretory pathway predominates and sAPPα is 10 times the amount of sAPPβ produced, increased sAPPα generated in the presence of the loop peptide may have compensated for the loss of sAPPβ. Thus, the loop-WT peptide seemingly had induced a shift from the β- to the α-secretory pathway.

As a control, we tested if the loop-WT or loop-mut peptide could have an influence on the subcellular localization of APP. Immunofluorescence analysis showed that none of the peptides altered APP localization (supplemental Fig. 3).

Because total secreted Aβ levels were found to have decreased as detected by Western blot analysis (Fig. 3*D*), we quantified the levels of Aβ species by ELISA using monoclonal antibodies specific for Aβ42 and Aβ40. The addition of the loop peptide significantly reduced Aβ40 in a concentration-dependent manner by 14, 35, and 45% (Fig. 3*A*). Aβ42 levels dropped significantly by 23, 51, and 57% for the respective loop peptide concentrations tested (Fig. 3*B*). This effect was due to altered APP processing because the substrate (full-length APP) levels were found unchanged (Fig. 3*C*). To prove whether the effects observed with the loop peptide depended on the disulfide bond arrangement or solely on the positively charged surface of the peptide, we performed the experiments described above with the loop-mut peptide. As shown in Figs. 2 and 3, the mutant peptide affected neither soluble APP levels nor Aβ40 or Aβ42 production in any direction.

Taken together, sAPPβ secretion (Fig. 2, *C* and *D*) and β-C-terminal fragment production were reduced (data not shown). Aβ40 and Aβ42 species decreased to a similar extent as the levels of sAPPβ (Fig. 3). To exclude a direct influence of the peptide on BACE enzyme activity, we assayed soluble BACE enriched from cell culture supernatant (20) in the presence of the loop-WT peptide (data not shown). Because we failed to detect any changes in activity (22) with or without the loop-WT peptide, and the peptide can specifically bind to APP18–350 (see Biacore data in Fig. 4 and NMR data in Fig. 5), we assume that the loop-WT peptide either competed for BACE binding to APP or had an allosteric effect.

The Loop-WT Peptide Binds to APP18–350—Using a surface plasmon resonance-based Biacore assay, we examined the ability of the loop-WT and loop-mut peptides to bind to APP18–350 in real time. We immobilized APP18–350 to a Biacore CM5 chip and applied different concentrations of the loop-WT or loop-mut peptide as a mobile analyte (Fig. 4). Binding of the loop-WT peptide to APP18–350 was measured in real time as an increase in resonance units. Injection of 2.2, 3.4, 5.7, and 6.8 μM concentrations of the loop-WT peptide led to the formation of complexes with immobilized APP18–350 as is visible from the large increase of resonance units (Fig. 4*A*). The rates of association and dissociation of the complexes were determined with the Biacore evaluation software (version 4.1). Based on the association and dissociation rates as given in Fig. 4, we have calculated the K_D to 7.0×10^{-7}. This indicates an affinity in the higher nanomolar range (Fig. 4). To investigate whether this binding is specific for peptide-protein interactions through the loop or simply through the basic residues, we also injected the control peptide onto the APP sensor chip. Binding of the loop-mut control peptide to APP was not observed (Fig. 4*B*). Because the loop-WT and loop-mut peptides differ only by the disulfide bridge, which is only present in the loop-WT peptide, we assume that the disulfide bond formed by Cys-98 and Cys-105 is essential for the interaction. We also conclude that the disulfide-bonded loop is of critical importance for the assembly of the homodimeric state of APP.

NMR Spectroscopy—The structures of GFLD (16), CuBD (25), and the Kunitz-type protease inhibitor (KPI) domain (26) were determined previously. However, none of these studies yielded any information about possible dimerization contact sites of APP.

Therefore, we used isotopically labeled APP18–350 and recorded $^{1}H,^{15}N$ correlation spectra of APP18–350 in the presence and absence of the loop-WT peptide (Fig. 5). We found severe spectral overlaps, in particular at ^{1}H and ^{15}N chemical shifts of around 7.8–8.5 and 118–126 ppm, respectively. The low dispersion in this part of the spectrum indicates that the protein contains unstructured regions that most likely reflect the increased mobility in the linkers connecting the three individual subdomains. Because of the large spectral overlap, we were not able to assign all resonances in this region. Superposition with the spectra obtained for the CuBD shows that the

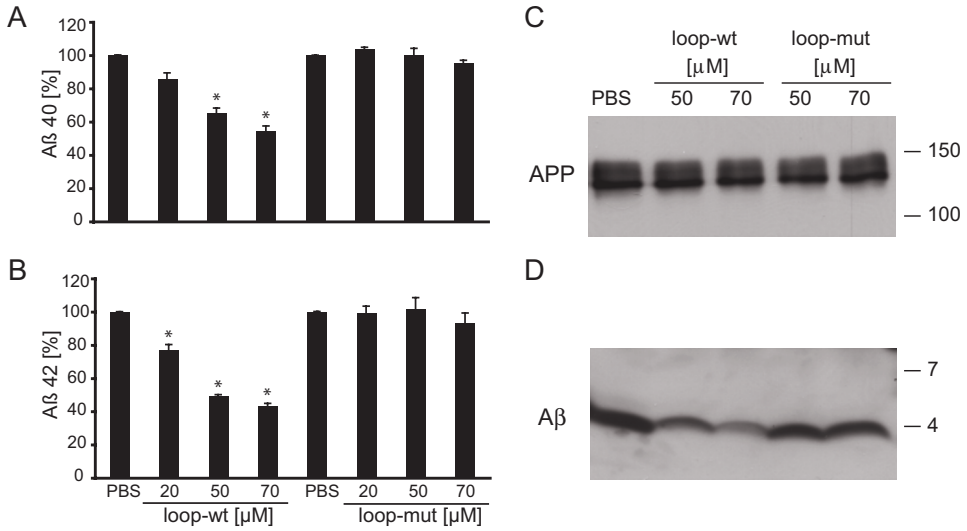

FIGURE 3. **SH-SY5Y cells treated with the loop peptide show a decreased Aβ production.** Quantification of Aβ40 (*A*) and Aβ42 (*B*) by ELISA revealed that only the loop-WT peptide, but not the loop-mut control peptide, decreased the formation of Aβ40 and Aβ42 in a concentration-dependent manner. The vehicle control (PBS) was set as 100% (means ± S.E., $n = 4–5$). *Asterisks* indicate significant differences with the control ($p < 0.001$, Student's *t* test). *C*, addition of the loop peptides did not alter APP expression or change APP maturation. APP was detected by Western blot analysis with antibody 22C11. *D*, only the presence of the loop-WT peptide led to a decrease in total Aβ levels. Aβ was detected with antibody W0-2.

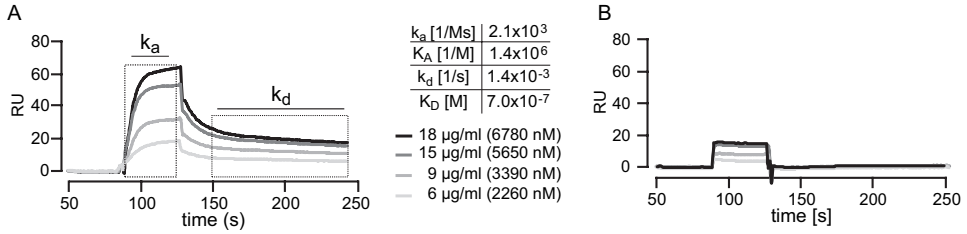

FIGURE 4. **Determination of binding specificity of the loop peptide by surface plasmon resonance spectroscopy.** Overlays of sensorgrams of loop-WT (*A*) and loop-mut (*B*) peptide injections onto APP18–350 are shown. APP18–350 from dimer-containing fractions of GPC was immobilized by NHS/EDC chemistry. Different concentrations of the loop-WT and loop-mut peptides were injected as indicated. Peptides diluted in running buffer were injected for 60 s, and the injection was stopped at 130 s. Only part of the dissociation phase is shown, but dissociation was further recorded for 10 min to calculate kinetics. Note that rectangular sudden changes in refractive indices for sensorgram *B* (injections of loop-mut peptide) are due to differences in the composition between buffer and protein solutions. k_a, association rate constant; k_d, dissociation rate constant; K_A, equilibrium association constant; K_D, equilibrium dissociation constant.

resonances of the CuBD in APP18–350 are not significantly perturbed. This indicates that the overall structure of the CuBD used for NMR studies is unchanged.

Interactions of APP18–350 with the Loop-WT Peptide Probed with Solution-state NMR—To identify the amino acids that are involved in the interaction between APP and the loop-WT peptide, we performed solution-state NMR experiments in the presence and absence of the loop-WT peptide using an equimolar ratio of peptide and protein. Larger concentrations of loop-WT peptide were prohibitive because they rapidly induced the precipitation of the protein. Fig. 5, *B* and *C*, represent specific parts of the spectrum. We observed significant chemical shift changes in all parts of the protein except the KPI domain. A quantitative analysis of all observed chemical shift changes is shown in Fig. 6. We found the largest chemical shift changes around the loop region affecting residues 65–130. However, residues in the CuBD and in the acidic amino acid-rich region between the CuBD and the KPI domain were also affected. In addition to those residues indicated in Fig. 5, *B* and *C*, a number of hydrophobic residues (Val-85, Val-86, Ala-126, and Lys-128) showed strong chemical shift changes (Fig. 6). In addition to the neutralization of the charge by the loop peptide, the exposure of hydrophobic side chains in the presence of the loop-WT peptide might explain the reduced solubility in the NMR titration experiments. The NMR data do not allow us to differentiate if APP18–350 dimerized in a head-to-tail or head-to-head arrangement. Thus, our biochemical data and published observations (7, 17) suggest that APP occurs in dimeric cis-forms. Nevertheless, in homophilic intercellular interaction studies, trans-interactions of APP family proteins were shown to promote cell-cell adhesion (18).

DISCUSSION

In this study, we have demonstrated that the N-terminal growth factor-like domain of APP can associate into SDS-labile and SDS-stable oligomers through the loop region as determined by GPC, SDS-PAGE, and cross-linking experiments. We have also demonstrated by using a synthetic peptide that mimicked the proposed β-hairpin loop of APP (16) that processing of APP by BACE is modulated in living cells if APP-expressing cells are incubated with the peptide. The cyclic peptide is stabilized by a disulfide bridge between Cys-98 and Cys-105 and drastically reduced levels of Aβ40 and Aβ42 secreted by living cells caused by attenuation of processing by β-secretase. Because the Cys-98–Cys-105 disulfide-bonded peptide specifically disrupted the SDS-labile APP18–350 dimers, we conclude that the peptide did not directly affect β-secretase but rather may change the APP conformation or allosterically affect APP processing. Although we cannot exclude that the loop-WT peptide can also bind to APP monomers, we conclude from the cross-linking and NMR experiments that it has a strong influence on the monomer-dimer transitions. The Biacore data indicate that only the disulfide-bonded loop-containing peptide directly binds to APP and that binding is entirely dependent on the presence of the oxidized thiol groups of the peptide.

To map distinct residues of APP18–350 that are involved in binding to the loop peptide, we recorded solution-state NMR heteronuclear single quantum correlation experiments. We find a very similar low resolution in the $^{1}H,^{15}N$ correlation experiments with and without the loop-WT peptide. This indicates that the overall structure of APP18–350 is largely unper-

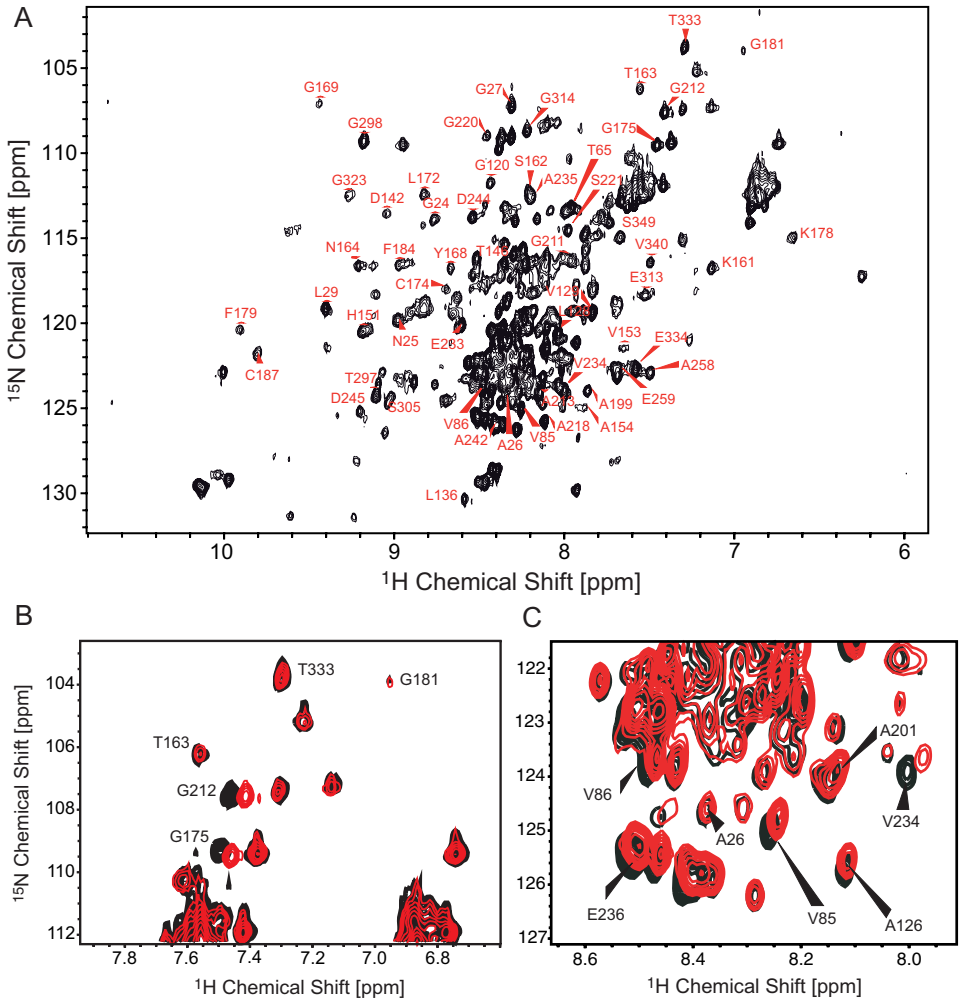

FIGURE 5. **Solution-state NMR of APP18–350 in the presence and absence of the loop peptide.** *A*, ^{1}H,^{15}N correlation spectrum of ^{15}N-labeled APP18–350 in the absence of the loop-WT peptide. *B* and *C*, ^{1}H,^{15}N heteronuclear single quantum correlation spectra of ^{15}N-labeled APP18–350 in the presence (*red*, molar ratio 1:1) and absence of the loop-WT peptide.

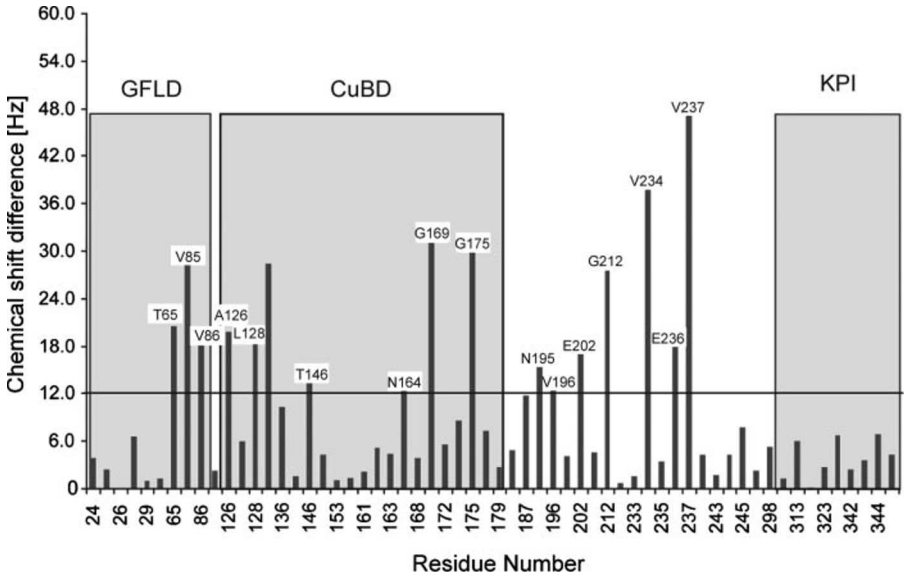

FIGURE 6. **NMR chemical shift changes of APP18–350 upon addition of the loop-WT peptide.** Individual subdomains of APP18–350 are indicated as *gray boxes*. The *horizontal bar* indicates chemical shift changes larger than 0.02 ppm, which can be considered significant. Upon addition of the loop-WT peptide, many resonances apart from the loop region were perturbed. Domain boundaries are 18–110 for GFLD, 123–180 for CuBD, and 287–350 for the KPI domain.

turbed, although conformational arrangements occur upon interaction with the loop-WT peptide leading to an altered processing of APP by the β-secretase. The individual domains (GFLD, CuBD, and KPI) are tumbling almost individually. Nevertheless, addition of the loop-WT peptide partially inhibited covalent cross-linking of APP18–350 dimers and affected β-secretase processing of membrane-bound APP, implying that APP-APP and APP-BACE interactions were somehow impaired. Also, upon addition of the loop-WT peptide, we detect small chemical shift changes in APP18–350 by NMR, which involve residues in almost all parts of the protein. In this case, the loop-WT peptide would specifically interact with a defined binding pocket in APP18–350 (only resonances in a certain region of APP18–350 should be affected), as the loop peptide itself is too small to interact with a large protein surface. Thus, we speculate based on NMR and biochemical data that the binding of the loop peptide interferes with APP dimerization through conformational changes in neighboring domains.

The NMR results agree qualitatively with the findings from the cross-linking experiment where ~20% of the protein could be fixed in the dimeric aggregation state indicating that the dimer may be rather short lived. As NMR is only sensitive to the ensemble average, we also cannot exclude that APP monomers are detected preferentially using NMR spectroscopy. At first sight, this contradicts the GPC experiments where monomers seem to be virtually absent. In general, higher oligomeric states are not easily observable by NMR as the increased molecular mass implies greater line widths and thus reduced sensitivity. NMR resonances are additionally broadened because of chemical exchange if these oligomers are conformationally heterogeneous. Under these circumstances, NMR spectroscopy detects APP monomers preferentially at an

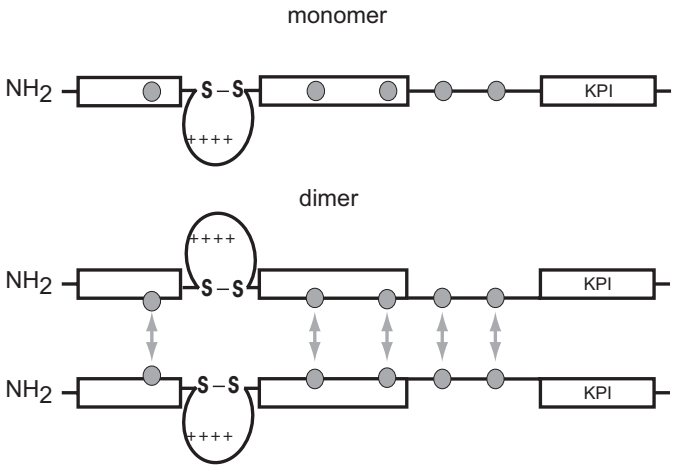

FIGURE 7. **Hypothetical oligomerization mechanism of APP.** The surface-exposed disulfide-bonded loop (Cys-98 and Cys-105) is crucial for loop-mediated homodimerization. Dimerization is shown to result from initial contacts mediated by the loop and in a more elongated manner by involving hydrophobic residues of neighboring domains. This is consistent with the observation that the chemical shift changes in NMR are relatively greater than expected by a simple binding of the loop-WT peptide to APP. *Boxes* represent the N-terminal APP domains GFLD followed by CuBD and the KPI domain. *Gray dots* represent conserved hydrophobic amino acid residues that are involved in conformational changes upon loop-WT peptide binding as determined by NMR.

effectively reduced sensitivity. A selective investigation of a specific oligomeric state that could possibly be separated using GPC is not feasible by NMR as all protein had to be pooled to yield a sufficiently high protein concentration. Alternatively, the NMR data might be indicative of a "molten globule" oligomeric state. The assembly of this oligomer might be driven by unspecific hydrophobic and electrostatic interactions. The individual components (GFLD, CuBD, and KPI) tumble relatively independently from one another. Interactions between different domains within the molecule could be mediated only by short-lived hydrophobic or electrostatic interactions without providing a specific protein interface for dimerization. This interpretation is in agreement with ^{15}N relaxation data that indicate that the individual subdomains tumble independently in the presence and absence of loop-WT peptide with a motional correlation time of $\tau_c = 8.4$ ns. This correlation time corresponds to an apparent molecular mass of ~11 kDa, which is close to the molecular mass of the individual subdomains of 10.6, 6.6, and 5.5 kDa for GFLD, CuBD, and KPI domain, respectively.

The homophilic binding mechanism of APP is still a subject of debate. Recently, we could provide evidence that APP forms dimers in living cells based on a fluorescence resonance energy transfer approach (7). We found that the transmembrane sequence of APP contains three consecutive G*XXX*G motifs providing a third dimerization site of APP and that mutations of this site within the membrane did not affect APP dimerization mediated by the ectodomain, *i.e.* the loop region investigated in this study and a second site spanning residues 448–465 (7). Importantly, the β-secretase activity remained unaffected by G*XXX*G mutants (7). An interesting aspect of the loop peptide studies reported here is that the loop peptide added to the cell culture medium drastically reduced β-secretase processing of membrane-bound APP and seemingly affected sAPPα vice versa. This can best be explained by structural perturbations resulting from direct binding of the loop peptide to APP.

Most importantly, APP-APP interactions depended on the Cys-98–Cys-105 disulfide bond of the loop peptide, whereas basic residues were less important. Indeed, there is increasing evidence favoring the possibility that this region encompassing the loop has a receptor function. From functional analyses it has been known that this region stimulated neurite outgrowth (27), promoted synaptogenesis (28), and activated MAPK (29). The presence of the Cys-98–Cys-105 disulfide bond was shown to be critical for neurite outgrowth and activated MAPK (27). A synthetic peptide covering the epitope of 22C11 competitively antagonized the action of monoclonal 22C11 (30). Collectively, these reports together with our findings may suggest that a ligand-induced conformational change in the APP extracellular domain may have a functional aspect.

The loop consists of several basic residues with only few conserved between APP family members and represents one of the heparin-binding sites of APP (31). Residues 96–110 were identified previously as forming part of a low affinity heparin-binding site (27, 32). The soluble form of APP (sAPPα) was reported to form a 2:1 complex with heparin (33). A model based on hypothetical conformations suggested either a parallel orientation of two APP monomers upon dimerization or an antiparallel orientation of two APP monomers joined by a high molecular mass heparin/heparan sulfate chain (33). In contrast, our data show that obviously a direct N-terminal interaction of APP-APP provides sufficient binding energy to give stable complexes.

The situation as it pertains to cell surface APP may prove more complex than inferred from the crystal structures of the recombinant APP28–123 (16). The loop-WT peptide can indeed lower the degree of APP dimerization and may be interacting in some way with a pre-existing dimer. Thus, our findings increase the evidence that the dimerization state of two APP molecules interacting through their loop regions has an impact on APP function. APP may be rather a preformed than ligand-induced dimer similar to the erythropoietin receptor and may be similarly loosely associated (34). We have evidence that the loop has a role in APP cellular localization.[4] Similar N-terminal disulfide-bonded loops have been identified as essential structures for sorting in chromogranin B (35), in proopiomelanocortin (36), and in the receptor tyrosine kinase MusK (37). As suggested by our biochemical and NMR data, we propose the mechanism depicted in Fig. 7. The initial recognition could be mediated by homomeric loop-loop complexes. These may then be stabilized by the formation of extended

[4] D. Kaden, P. Voigt, L. M., Munter, M. Schaefer, G. Multhaup, manuscript in preparation.

intermolecular duplexes through hydrophobic residues that are conserved between APP and amyloid precursor-like proteins.

If APP is transported once to the cell surface as a dimer, it may then undergo a heparin-induced conformational change to achieve the status of an active growth factor. Identification of the long-sought growth factor receptor(s) of the GFLD of APP should then be possible in the presence of a ligand bound to the APP loop region, such as heparin.

Acknowledgments—We thank P. Paganetti for kindly providing antibody 879 and Rüdiger Pipkorn for initial synthesis of peptides.

REFERENCES

1. Reinhard, C., Hebert, S. S., and De Strooper, B. (2005) *EMBO J.* **24,** 3996–4006
2. Esch, F. S., Keim, P. S., Beattie, E. C., Blacher, R. W., Culwell, A. R., Oltersdorf, T., McClure, D., and Ward, P. J. (1990) *Science* **248,** 1122–1124
3. Sinha, S., and Lieberburg, I. (1999) *Proc. Natl. Acad. Sci. U. S. A.* **96,** 11049–11053
4. Sisodia, S. S., Koo, E. H., Beyreuther, K., Unterbeck, A., and Price, D. L. (1990) *Science* **248,** 492–495
5. Vassar, R., Bennett, B. D., Babu-Khan, S., Kahn, S., Mendiaz, E. A., Denis, P., Teplow, D. B., Ross, S., Amarante, P., Loeloff, R., Luo, Y., Fisher, S., Fuller, J., Edenson, S., Lile, J., Jarosinski, M. A., Biere, A. L., Curran, E., Burgess, T., Louis, J. C., Collins, F., Treanor, J., Rogers, G., and Citron, M. (1999) *Science* **286,** 735–741
6. Gu, Y., Misonou, H., Sato, T., Dohmae, N., Takio, K., and Ihara, Y. (2001) *J. Biol. Chem.* **276,** 35235–35238
7. Munter, L. M., Voigt, P., Harmeier, A., Kaden, D., Gottschalk, K. E., Weise, C., Pipkorn, R., Schaefer, M., Langosch, D., and Multhaup, G. (2007) *EMBO J.* **26,** 1702–1712
8. Sherrington, R., Rogaev, E. I., Liang, Y., Rogaeva, E. A., Levesque, G., Ikeda, M., Chi, H., Lin, C., Li, G., Holman, K., Tsuda, T., Mar, L., Foncin, J.-F., Bruni, A. C., Montesi, M. P., Sorbi, S., Rainero, I., Pinessi, L., Nee, L., Chumakov, I., Pollen, D., Brookes, A., Sanseau, P., Polinsky, R. J., Wasco, W., da Silva, H. A. R., Haines, J. L., Pericak-Vance, M. A., Tanzi, R. E., Roses, A. D., Fraser, P. E., Rommens, J. M., and St George-Hyslop, P. H. (1995) *Nature* **375,** 754–760
9. Yu, C., Kim, S. H., Ikeuchi, T., Xu, H., Gasparini, L., Wang, R., and Sisodia, S. S. (2001) *J. Biol. Chem.* **276,** 43756–43760
10. Daigle, I., and Li, C. (1993) *Proc. Natl. Acad. Sci. U. S. A.* **90,** 12045–12049
11. Kitaguchi, N., Takahashi, Y., Oishi, K., Shiojiri, S., Tokushima, Y., Utsunomiya, T., and Ito, H. (1990) *Biochim. Biophys. Acta* **1038,** 105–113
12. Dulubova, I., Ho, A., Huryeva, I., Sudhof, T. C., and Rizo, J. (2004) *Biochemistry* **43,** 9583–9588
13. Beher, D., Hesse, L., Masters, C. L., and Multhaup, G. (1996) *J. Biol. Chem.* **271,** 1613–1620
14. Ferguson, K. M., Darling, P. J., Mohan, M. J., Macatee, T. L., and Lemmon, M. A. (2000) *EMBO J.* **19,** 4632–4643
15. Marambaud, P., Shioi, J., Serban, G., Georgakopoulos, A., Sarner, S., Nagy, V., Baki, L., Wen, P., Efthimiopoulos, S., Shao, Z., Wisniewski, T., and Robakis, N. K. (2002) *EMBO J.* **21,** 1948–1956
16. Rossjohn, J., Cappai, R., Feil, S. C., Henry, A., McKinstry, W. J., Galatis, D., Hesse, L., Multhaup, G., Beyreuther, K., Masters, C. L., and Parker, M. W. (1999) *Nat. Struct. Biol.* **6,** 327–331
17. Scheuermann, S., Hambsch, B., Hesse, L., Stumm, J., Schmidt, C., Beher, D., Bayer, T. A., Beyreuther, K., and Multhaup, G. (2001) *J. Biol. Chem.* **276,** 33923–33929
18. Soba, P., Eggert, S., Wagner, K., Zentgraf, H., Siehl, K., Kreger, S., Lower, A., Langer, A., Merdes, G., Paro, R., Masters, C. L., Muller, U., Kins, S., and Beyreuther, K. (2005) *EMBO J.* **24,** 3624–3634
19. Wang, Y., and Ha, Y. (2004) *Mol. Cell* **15,** 343–353
20. Schmechel, A., Strauss, M., Schlicksupp, A., Pipkorn, R., Haass, C., Bayer, T. A., and Multhaup, G. (2004) *J. Biol. Chem.* **279,** 39710–39717
21. Ida, N., Hartmann, T., Pantel, J., Schroder, J., Zerfass, R., Forstl, H., Sandbrink, R., Masters, C. L., and Beyreuther, K. (1996) *J. Biol. Chem.* **271,** 22908–22914
22. Westmeyer, G. G., Willem, M., Lichtenthaler, S. F., Lurman, G., Multhaup, G., Assfalg-Machleidt, I., Reiss, K., Saftig, P., and Haass, C. (2004) *J. Biol. Chem.* **279,** 53205–53212
23. Hilbich, C., Monning, U., Grund, C., Masters, C. L., and Beyreuther, K. (1993) *J. Biol. Chem.* **268,** 26571–26577
24. Salzmann, M., Pervushin, K., Wider, G., Senn, H., and Wuthrich, K. (1998) *Proc. Natl. Acad. Sci. U. S. A.* **95,** 13585–13590
25. Barnham, K. J., McKinstry, W. J., Multhaup, G., Galatis, D., Morton, C. J., Curtain, C. C., Williamson, N. A., White, A. R., Hinds, M. G., Norton, R. S., Beyreuther, K., Masters, C. L., Parker, M. W., and Cappai, R. (2003) *J. Biol. Chem.* **278,** 17401–17407
26. Hynes, T. R., Randal, M., Kennedy, L. A., Eigenbrot, C., and Kossiakoff, A. A. (1990) *Biochemistry* **29,** 10018–10022
27. Small, D. H., Nurcombe, V., Reed, G., Clarris, H., Moir, R., Beyreuther, K., and Masters, C. L. (1994) *J. Neurosci.* **14,** 2117–2127
28. Morimoto, T., Ohsawa, I., Takamura, C., Ishiguro, M., and Kohsaka, S. (1998) *J. Neurosci. Res.* **51,** 185–195
29. Greenberg, S. M., Qiu, W. Q., Selkoe, D. J., Ben-Itzhak, A., and Kosik, K. S. (1995) *Neurosci. Lett.* **198,** 52–56
30. Okamoto, T., Takeda, S., Murayama, Y., Ogata, E., and Nishimoto, I. (1995) *J. Biol. Chem.* **270,** 4205–4208
31. Small, D. H., Nurcombe, V., Moir, R., Michaelson, S., Monard, D., Beyreuther, K., and Masters, C. L. (1992) *J. Neurosci.* **12,** 4143–4150
32. Multhaup, G. (1994) *Biochimie* (*Paris*) **76,** 304–311
33. Gralle, M., Oliveira, C. L., Guerreiro, L. H., McKinstry, W. J., Galatis, D., Masters, C. L., Cappai, R., Parker, M. W., Ramos, C. H., Torriani, I., and Ferreira, S. T. (2006) *J. Mol. Biol.* **357,** 493–508
34. Wilson, I. A., and Jolliffe, L. K. (1999) *Curr. Opin. Struct. Biol.* **9,** 696–704
35. Chanat, E., Weiss, U., Huttner, W. B., and Tooze, S. A. (1993) *EMBO J.* **12,** 2159–2168
36. Cool, D. R., Normant, E., Shen, F., Chen, H. C., Pannell, L., Zhang, Y., and Loh, Y. P. (1997) *Cell* **88,** 73–83
37. Stiegler, A. L., Burden, S. J., and Hubbard, S. R. (2006) *J. Mol. Biol.* **364,** 424–433